# Computation and comparison of the stable Northeastern US marine boundary layer

Lawrence C. Cheung[1]
*Sandia National Laboratories, Livermore, CA, 94550, USA*

Alan S. Hsieh[2]
*Sandia National Laboratories, Albuquerque, NM, 87185, USA*

Michael J. Brazell[3] and Ganesh Vijayakumar[4]
*National Renewable Energy Laboratory, Golden, CO, 80401, USA*

**Large eddy simulations are used in this study to calculate stably stratified offshore boundary layers in the Northeastern US and to compare their behavior with previous neutral and unstable cases. Stable boundary layer conditions, with wind speeds from 5 m/s to 15 m/s, are chosen to match experimental measurements collected near Nantucket Sound. The characteristics of the stable boundary layers, including mean profiles, wind spectra, and turbulence statistics are compared to the neutral and unstable cases. This study also examines the accuracy and performance of two atmospheric boundary layer solvers, the unstructured Nalu-Wind code and adaptive mesh refinement approach of AMR-Wind, in calculating the stable marine boundary layer.**

## I. Nomenclature

| | | |
|---|---|---|
| $\alpha$ | = | Wind shear exponent |
| $\Delta$ | = | Mesh spacing in the horizontal direction |
| $i$ | = | Directional index for velocity components *u*, *v*, *w* |
| $f$ | = | Temporal frequency |
| $f_{max}$ | = | Maximum resolvable frequency in LES computations |
| $g$ | = | Gravitational acceleration |
| $\kappa$ | = | Kolmogorov constant |
| $L$ | = | Obukhov length scale |
| $\sigma_i$ | = | Wind velocity variance for velocity component $i$ |
| $S_i$ | = | Wind spectra for the velocity component $i$ |
| $u_\tau$ | = | Friction velocity |
| $T_0$ | = | Surface temperature |
| $\overline{U_h}$ | = | Mean horizontal velocity |
| $z$ | = | Vertical elevation coordinate |

## II. Introduction

The planned installation of several offshore wind energy plants in the United States has highlighted the need to properly understand the wind resource and atmospheric characteristics of the US Atlantic Coast. Several atmospheric

[1] Principal member of technical staff, Thermal/Fluid Science & Engineering, AIAA member
[2] Postdoctoral appointee, Wind Energy Technologies Department, AIAA member.
[3] Researcher III, High-Performance Algorithms and Complex Fluids, AIAA member.
[4] Researcher III, Mechanical Engineering, AIAA member.

phenomena particular to this region, such as coastal low-level jets or seasonal Nor'easters, have the potential to substantially impact the operation and power production of offshore wind plants. Of particular interest to the current study is the atmospheric stability of the marine boundary layer in the Northeastern US.

Atmospheric stability plays a large role in determining the power production of wind plants because it directly affects the vertical distribution of momentum and turbulent energy in the atmospheric boundary layer (ABL). The differences between the stable, neutral, or unstable stratified ABL can lead to large changes in wind speed or turbulence profiles, and ultimately change the operation of wind turbines. Atmospheric stability may also play a role in the formation of low-level jets [1] and cause increased fatigue loads on offshore wind turbines.

Several recent measurement campaigns have provided data to understand the ABL and wind characteristics for potential offshore wind farms in the Northeastern US. Pichugina *et al.* [2] measured the wind profiles and vertical shear profiles in the Gulf of Maine using a ship-borne lidar approach. Analysis of measured data sets from Nantucket Sound by Archer *et al.* [3] showed a predominance of low-shear, unstable conditions at the site. However, strong seasonal variations and stratification changes due to diurnal variation were also observed.

In addition to these measurements, large eddy simulations (LES) have also been used to study ABL stability characteristics. Recent work by Kaul *et al.* [4] has shown that LES computations using Nalu-Wind can capture the neutrally and convectively unstable onshore ABL. Previous simulations by Cheung *et al.* [5] successfully replicated the unstable and neutral ABL corresponding to the Cape Wind meteorological tower measurements [3] and showed the effects of surface heating on atmospheric stratification. Additional LES computations [6] have also previously explored stable conditions of onshore boundary layers, such as the GABLS1 boundary layer [7]. However, a complete comparison including offshore stable ABL conditions has yet to be completed.

### A. Study objectives

In this study, we plan to accomplish the following set of objectives. First, a series of stable marine boundary layer simulations will be computed which match the atmospheric properties measured by Archer *et al.* [3] Secondly, the statistics of these stable ABL will be compared with the neutral and unstable conditions previously studied in [5], to determine the influence of stratification. These statistics include not only the mean boundary layer quantities, but wind spectra at multiple heights and turbulent length scales. The statistical quantities from the large eddy simulations will also be compared against turbulence models currently used in the literature. Finally, two numerical approaches will be compared in this study: the unstructured, incompressible Navier-Stokes solver Nalu-Wind and a similar approach based on adaptive mesh refinement (AMR-Wind). The accuracy and efficiency of both methods will be reported.

## III. Methodology

### A. Experimental measurements

Conditions for the large eddy simulations in this study are chosen to match the data collected by the Cape Wind meteorological tower in Nantucket Sound. As described by Archer *et al.* [3], these measurements include wind speed, direction, temperature, and barometric measurements at heights of 20m, 41m, and 60m above the mean water level. This data also captured diurnal and seasonal variation in atmospheric behavior over several years from 2003 to 2011. Although the study found that the marine boundary layer was predominantly unstable at that location, there were also noticeable differences in the mean profiles between the stability states.

**Table 1**. Measured ABL conditions from Cape Wind data

| Stability | Wind speed [m/s] | Wind dir [deg] | Turbulence Intensity |
|---|---|---|---|
| **Stable** | 5 | 225 | 0.045 |
| **Stable** | 10 | 225 | 0.050 |
| **Stable** | 15 | 225 | 0.060 |
| **Neutral** | 5 | 225 | 0.055 |
| **Neutral** | 10 | 225 | 0.055 |
| **Neutral** | 15 | 225 | 0.065 |
| **Unstable** | 5 | 315 | 0.080 |
| **Unstable** | 10 | 315 | 0.075 |
| **Unstable** | 15 | 315 | 0.090 |

From the Cape Wind measurements, three wind speeds (5 m/s, 10 m/s, and 15 m/s) were chosen to cover the range of conditions observed through the 20m sonic anemometer. The corresponding median TI values and wind directions were also selected at wind speed. A summary of the targeted ABL conditions for all stability states (stable, neutral, and unstable) is shown in Table 1.

### B. Computational methodology

In this study, two different computational codes will be used for the large eddy simulations of the offshore ABL. Both LES solvers were developed as a part of the US Department of Energy Exawind and Exascale computing project and contain similar functionality. The first solver, Nalu-Wind [8, 9], uses an unstructured, finite volume approach to solve the incompressible Navier-Stokes equations with a low-Mach number approximation and a Boussinesq buoyancy model, along with the Coriolis forcing term. Nalu-Wind was previously used by Cheung *et al*. [5] for the computation of the neutral and unstable ABL at Cape Wind, and has also been demonstrated for blade-resolved simulations of wind turbines [8]. Additional details on the numerical schemes and computational methodology in Nalu-Wind can be found in the online documentation [10].

The second code, AMR-Wind [11], is a block-structured adaptive-mesh, variable-density, incompressible Navier-Stokes solver. AMR-Wind is built on top of the AMReX [12, 13] software framework and the discretization is based on IAMR [14, 15]. The discretization uses a second-order projection methodology for enforcing the incompressibility constraint. Advection terms are handled using a high-order Godunov explicit integration scheme while diffusion terms are handled using a second-order finite-difference method. Similar to Nalu-Wind there is support for Boussinesq buoyancy and Coriolis forcing.

For all ABL computations in this study, both solvers will use identical settings and parameters to ensure uniformity in the subsequent comparisons and will also match the previously used procedures. Both codes will use a one-equation, constant-coefficient turbulent kinetic energy model for the calculation of the turbulent subgrid scale stresses. Details behind the applied boundary conditions and initial conditions can be found in [5].

As in the previous study, two domain sizes -- a large domain and a small domain -- will be for the computation of each ABL condition. The large domain, up to 6 km × 6 km × 1 km, will be used for the full scale runs and gathering of ABL statistics. A smaller 1.5 km × 1.5 km × 1 km domain will be used to determine the appropriate surface roughness and heat flux to reach the desired stable condition. For the stable ABL cases, an initial mesh spacing of 10 m × 10 m × 6 m will be used in the computations and adjusted so that the peak wind spectra and the relevant turbulent scales will be captured.

## IV. Preliminary results

An initial comparison between the stable and neutral/unstable ABL behavior can be done using the preliminary results obtained for the stable 5m/s case with Nalu-Wind on the small domain. Differences in the mean flow and wind spectra are readily apparent and described in the following sections.

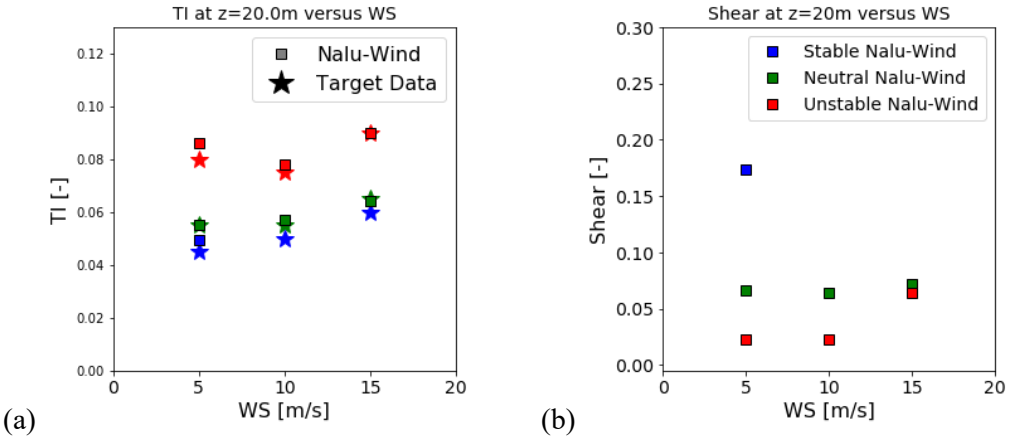


**Figure 1. (a) Comparison of the computed versus target TI conditions. (b) Shear exponent versus wind speed (WS) for stable, neutral, and unstable conditions.**

### A. Mean flow statistics

The comparison between the time averaged, horizontally averaged turbulence intensity and shear exponent is shown in Figure 1. Generally speaking, the turbulence levels for the stable ABL conditions are close to neutral values, around 5-6% TI), and the Nalu-Wind computed TI closely matched the measured target. However, a larger difference is seen in the averaged shear exponent $\alpha$ in Figure 1(b). For the 5 m/s case, the stable ABL case had a shear exponent $\alpha = 0.17$ much higher than the neutral or stable cases.

A similar conclusion can be drawn by examining the mean TI and velocity profiles in Figure 2. Below $z$=200m, the decay of the turbulence profile for the stable case closely resembles the neutral case. However, the much higher shear in the stable ABL is evident in the velocity profile in Figure 2(b).

The stable 5 m/s case also displays a stronger veer and temperature gradient compared to the neutral and stable cases. In Figure 3(a), the wind direction change over the first 200m for the stable ABL is approximately twice as large as the neutral case. While the unstable case has negligible veer compared to the other cases, the temperature gradient near the ocean surface is comparable to the stable case.

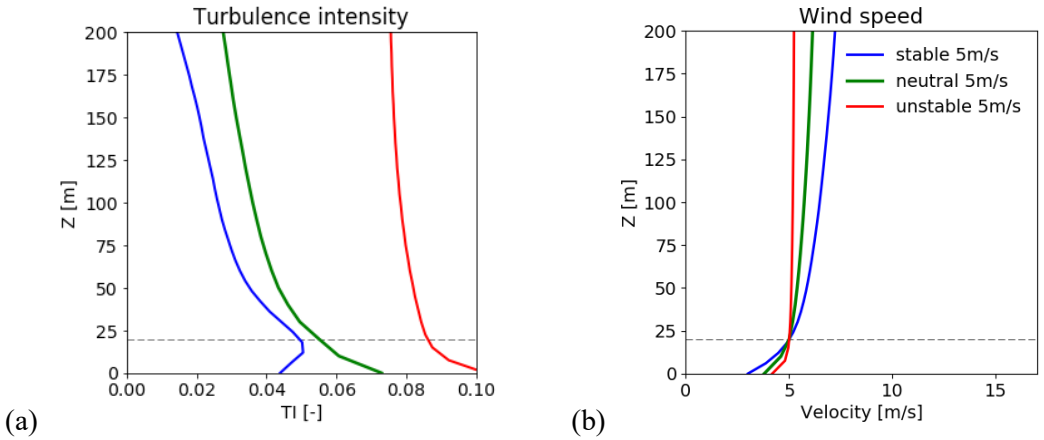


**Figure 2. (a) Comparison of the TI profiles for stable, neutral, and unstable 5 m/s cases. (b) Comparison of the mean velocity profile for stable, neutral, and unstable 5 m/s cases.**

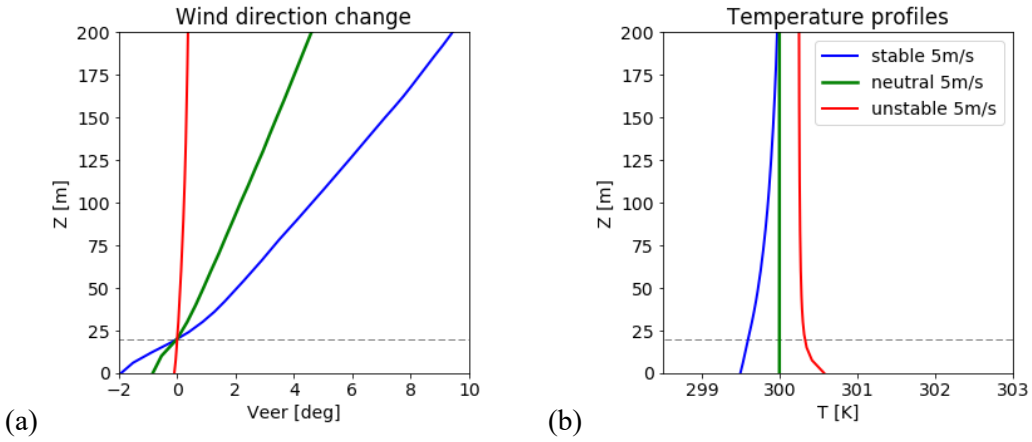


**Figure 3. (a) Wind veer. (b) Temperature profiles**

The stratification of the offshore ABL cases can be quantified through the Obhukov length $L$, which can be approximated as

$$L \approx -\frac{u_\tau^3}{\frac{\kappa g}{T_0}\overline{w'T'}}, \tag{1}$$

where $\overline{w'T'}$ is the vertical temperature flux, $T_0$ is the surface temperature, $u_\tau$ the friction velocity, $\kappa$ is the Kolmogorov constant, and $g$ is the gravitational acceleration. Here we use the stability classification boundaries defined in [16], where very unstable is defined as $-200 < L < 0$, unstable as $-1000 < L < -200$, stable as $200 < L < 1000$, very stable as $0 < L < 200$, and neutral as $|L| > 1000$. When plotted in Figure 4, the current 5 m/s ABL case is classified as stable, compared to the very unstable 5 m/s ABL case.

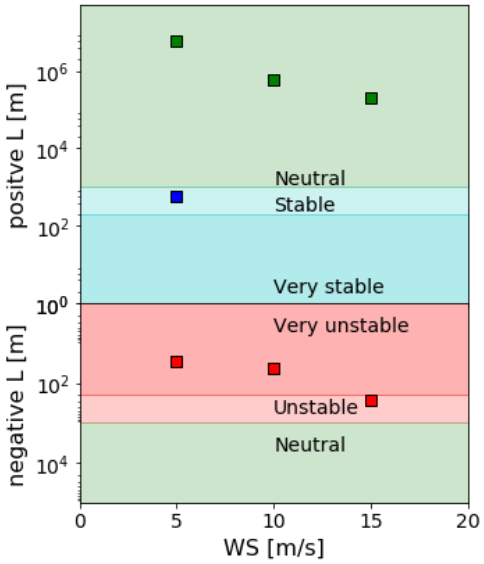


**Figure 4. The classification of atmospheric stability based on Obukhov length**

### B. Comparison of wind spectra

In the final set of comparisons, we compare the turbulent spectra from the stable case with other stratifications. Here the wind spectra $S_i(f)$ for frequency $f$ can be related to the wind variances $\sigma_i$ using the equation

$$\int_0^\infty S_i(f)\ \mathrm{d}f = \sigma_i^2, \tag{2}$$

given the index $i = u, v, w$ for each of the directions. In addition to the spectra computed from the Nalu-wind results, we also can explore how well the Kaimal model [17] captures the spectra for different atmospheric stabilities. Here the nondimensionalized Kaimal spectral model is calculated as

$$\frac{fS_i}{u_\tau^2} = \frac{a_i[fz/\overline{U}]}{(1 + b_i[fz/\overline{U}]^{\alpha_i})^{\beta_i}} \tag{3}$$

where the parameters $a_i, b_i, \alpha_i, \beta_i$ are the standard Kaimal coefficients used in [5] and [18]. The maximum resolvable frequency $f_{max}$ for the Nalu-wind computations can be estimated as $f_{max} = 0.6\overline{U}_h/(8\Delta)$, where $\overline{U}_h$ is the mean horizontal velocity and $\Delta = 10\sqrt{2}$ m is the mesh spacing in the longitudinal direction.

The stable, neutral, and unstable wind spectra for the 5 m/s ABL cases, from both the Nalu-wind LES and the Kaimal model, are shown in Figure 5. Up to the frequency $f_{max}$, the Kaimal model agrees best with the neutral ABL case. For the stable ABL case, the Kaimal model over-predicts the energy in all three components. On the other hand, the spectra for the unstable ABL displays much higher low frequency energy compared to the Kaimal model.

Finally, the behavior of the longitudinal wind spectra with height is illustrated in Figure 6. The unstable ABL case shows minimal change in spectra from z=20m to z=60m, while both the spectra in the stable and neutral case show decay from the predicted Kaimal at higher elevations. This behavior is expected and can be explained in terms of the stratification effects. The presence of surface heating in the unstable case enhances the vertical mixing and allows energy to be transported easily through different elevations. On the other hand, stable stratification inhibits vertical mixing, and the turbulent decay with elevation is strongest in this case.

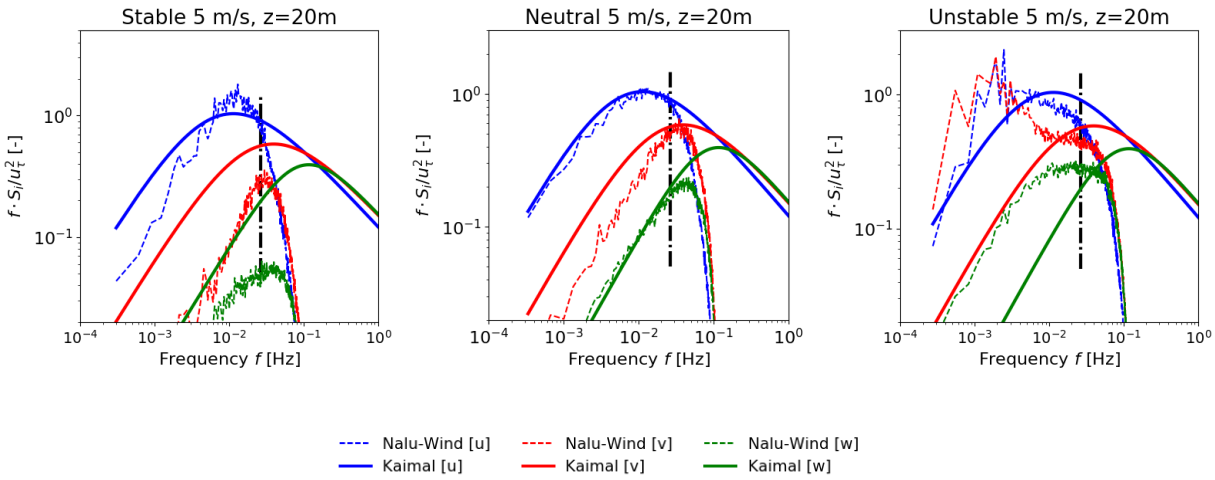


**Figure 5. Calculated and Kaimal model spectra at height $z = 20$m for the stable, neutral, and unstable 5m/s ABL cases. The vertical dashed line corresponds to the maximum resolvable frequency $f_{max}$.**

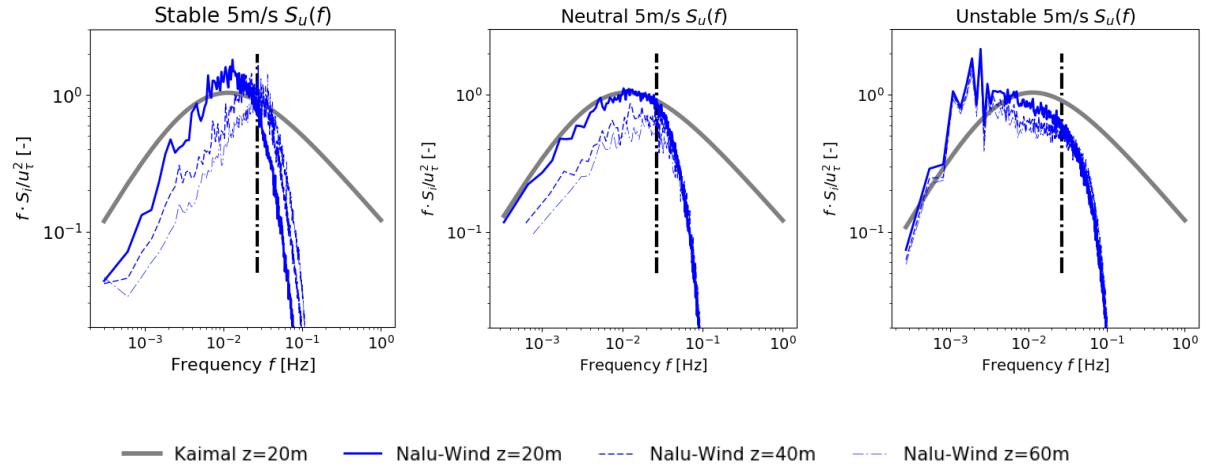


**Figure 6. The longitudinal wind spectra for the stable, neutral, and unstable 5m/s ABL cases at heights z=20m, 40m, and 60m. The vertical dashed line corresponds to the maximum resolvable frequency $f_{max}$.**

## V. Conclusion

In this study, large eddy simulations are used to calculate and compare the behavior of stable marine boundary layers near the northeast US coast. Both Nalu-Wind and AMR-Wind are used to simulate the stable ABL's with speeds from 5 m/s to 15 m/s and matching the atmospheric properties by Archer *et al.* The statistics and turbulence properties of these boundary layers are then compared to previously computed neutral and unstable conditions at the same location. The accuracy and efficiency of both the Nalu-Wind and AMR-Wind solvers are also compared.

## Acknowledgments

This research was supported by the Wind Energy Technologies Office of the US Department of Energy Office of Energy Efficiency and Renewable Energy. Sandia National Laboratories is a multimission laboratory managed and operated by National Technology & Engineering Solutions of Sandia, LLC, a wholly owned subsidiary of Honeywell International Inc., for the U.S. Department of Energy's National Nuclear Security Administration under contract DE-

NA0003525. The views expressed in the article do not necessarily represent the views of the U.S. Department of Energy or the United States Government. SAND2020-5758A

## References

[1] C. G. Nunalee and S. Basu, "Mesoscale modeling of coastal low-level jets: implications for offshore wind resource estimation," *Wind Energy*, vol. 17, no. 8, pp. 1199-1216, 2014.

[2] Y. Pichugina, W. Brewer, R. Banta, A. Choukulkar, C. Clack, M. Marquis, B. McCarty, A. Weickmann, S. Sandberg, R. Marchbanks and R. Hardesty, "Properties of the offshore low level jet and rotor layer wind shear as measured by scanning Doppler Lidar," *Wind Energy*, vol. 20, no. 6, pp. 987-1002, 2017.

[3] C. Archer, B. Colle, D. Veron, F. Veron and M. J. and Sienhiewicz, "On the predominance of unstable atmospheric conditions in the marine boundary layer offshore of the US northeastern coast," *Journal of Geophysical Research: Atmospheres*, vol. 121, no. 15, pp. 8869-8885, 2016.

[4] C. Kaul, S. Ananthan, M. Churchfield, J. Mirocha, L. Berg and R. Rai, "Large eddy simulations of idealized atmospheric boundary layers using Nalu-Wind," in *NAWEA WindTech Conference Proceedings, Oct. 13-16, 2019*, Amherst, MA, 2019.

[5] L. Cheung, C. Kaul, M. Blaylock, A. Hsieh and M. Churchfield, "Large eddy simulations of the Northeastern US Coastal marine boundary layer," in *Torque Conference Proceedings*, Delft, Netherlands, 2020.

[6] P. P. Sullivan, J. C. Weil, E. G. Patton, H. J. Jonker and a. D. V. Mironov, "Turbulent winds and temperature fronts in large-eddy simulations of the stable atmospheric boundary layer," *Journal of the Atmospheric Sciences*, vol. 73, no. 4, pp. 1815-1840, 2016.

[7] R. Beare, M. Macvean, A. Holtslag, J. Cuxart, I. Esau, J. Golaz, M. Jimenez, M. Khairoutdinov, B. Kosovic, D. Lewellen and T. Lund, "An intercomparison of large-eddy simulations of the stable boundary layer," *Boundary-Layer Meteorology*, vol. 118, no. 2, pp. 247-272, 2006.

[8] M. A. Sprague, S. Ananthan, G. Vijayakumar and M. Robinson, "ExaWind: A multi-fidelity modeling and simulation environment for wind energy," in *NAWEA WindTech Conference Proceedings, Oct. 13-16, 2019*, Amherst, MA, 2019.

[9] S. P. Domino, "Sierra Low Mach Module: Nalu Theory Manual 1.0," Sandia National Laboratories SAND2015-3107W, 2015.

[10] "Nalu-Wind Documentation," [Online]. Available: https://nalu-wind.readthedocs.io/en/latest/index.html.

[11] [Online]. Available: https://github.com/Exawind/amr-wind.

[12] [Online]. Available: https://amrex-codes.github.io/amrex.

[13] W. Zhang, A. A. V. B. J. Bell, J. Blaschke, C. Chan, M. Day, B. Friesen, K. Gott, D. Graves and M. Katz, "AMReX: a framework for block-structured adaptive mesh refinement," *Journal of Open Source Software*, vol. 4, no. 37, 2019.

[14] A. S. Almgren, J. B. Bell, P. Colella, L. H. Howell and a. M. L. Welcome, "A conservative adaptive projection method for the variable density incompressible Navier–Stokes equations," *Journal of computational Physics*, vol. 142, no. 1, pp. 1-46, 1998.

[15] [Online]. Available: https://amrex-codes.github.io/IAMR.

[16] M. Motta, R. J. Barthelmie and a. P. Vølund, "The influence of non-logarithmic wind speed profiles on potential power output at Danish offshore sites," *Wind Energy: An International Journal for Progress and Applications in Wind Power Conversion Technology*, vol. 8, no. 2, pp. 219-236, 2005.

[17] J. C. J. Kaimal, "Turbulence spectra, length scales and structure parameters in the stable surface layer," *Boundary-Layer Meteorology*, vol. 4, no. 1-4, pp. 289-309, 1973.

[18] E. Cheynet, J. B. Jakobsen and C. Obhrai, "Spectral characteristics of surface-layer turbulence in the North Sea," *Energy Procedia*, vol. 137, pp. 414-427, 2017.